Numerical investigation of soot formation and radiative heat transfer in ethylene microgravity laminar boundary layer diffusion flames.

J.Contreras[1], J.L. Consalvi[*, 1], A. Fuentes[2], F. Liu[3]

[1] Aix-Marseille Université, IUSTI/UMR CNRS 7343, 5 rue E. Fermi, 13453 Marseille Cedex 13, France.
[2] Departamento de Industrias, Universidad Técnica Federico Santa María, Av. España 1680, Valparaíso, Chile.
[3] Measurement Science and Standards, National Research Council of Canada, 1200 Montreal Road, Ottawa, Ontario, Canada K1A 0R6.

Abstract

The aim of the present study is to assess the capability of different approximate radiative property models to predict the flame structure and the radiative quenching at the trailing edge of a microgravity ethylene laminar boundary layer (LBL) diffusion flame. The reference solution is computed by using a Statistical Narrow Band Correlated–k (SNBCK) Wide Band model coupled to the Discrete Ordinate Method (DOM). Three approximate radiative models are considered: i) the gray soot model which considers a Planck mean absorption coefficient for soot, ii) the Planck-mean model which considers a Planck mean absorption coefficient for gas and soot, and iiii) the Optically-Thin Approximation (OTA). These radiative models are implemented in a 2D CFD model in order to simulate an ethylene microgravity LBL diffusion flame burning in air. The numerical model is based on a comprehensive kinetic mechanism, and a soot model consisting of inception as a result of the collision of two pyrene molecules, heterogeneous surface growth and oxidation following the hydrogen abstraction acetylene addition (HACA) mechanism, soot particle coagulation, and PAH surface condensation. Model results show that soot radiation represents 45% of the total radiative loss and plays a crucial role in the flame quenching at the trailing edge. The ranking of the model in order of decreasing accuracy is the following: 1) the Gray soot, 2) the Planck mean, and 3) the OTA. None of these approximate models should be used if a reliable description of the flame structure and the phenomenon of flame quenching at the trailing edge is desired.

Introduction

Extinction of diffusion flames is important from a fundamental, but also from a practical point of view. Many aspects of combustion, such as combustion efficiency in engines, boilers and furnaces, generation of pollutants, and fire safety, are directly affected by flame extinction. Extinction is described in terms of the Damkohler number, Da, defined as the ratio of the characteristic flow time to the chemical reaction time. Two modes of extinction have been established. For low Damkohler numbers, characterized by short residence times, the extinction mode is called kinetic extinction and can be induced by high scalar dissipation rates, low reactant concentrations or low mass flow rates. Conversely, for high Damkohler numbers the residence times are long and the radiation heat loss induced extinction can occur. As the Damkohler number increases, the energy loss through radiation cools the flame, decreasing the temperature and leading to a reduction of the reaction rates. Extinction takes place when the excessive heat loss significantly lowers the temperatures and hence reaction rates such that the flame can no longer sustain itself [1,2]. The conditions for radiative extinction can be more easily achieved in microgravity environments, where buoyancy induced flow acceleration (related to strain) is absent and radiation heat loss can be the predominant heat transfer mechanism, even for small flames [3,4].

Because radiative extinction occurs at long residence times (Large Da), low velocity gas flows under microgravity conditions are ideal to explore radiative extinction [5,6] and to study the effects of transport in soot production and oxidation [7]. Laminar boundary layer diffusion flames over a plate are a good candidate to study both soot production and radiative quenching of the flame at the trailing edge and some works have been conducted towards this goal in the 15 last years or so [7-11]. Furthermore, this configuration is of extreme importance for investigation of spacecraft fire safety [3,5,6,11]. The present study aims to evaluate the influence of different radiation models in the prediction of flame structure, soot production, and radiative quenching in a microgravity laminar boundary layer diffusion flame fuelled with ethylene. In order to accomplish this task, a microgravity LBL diffusion flame was simulated by using detailed CFD model with the Statistical Narrow Band Correlated –k (SNBCK) Wide Band model coupled to the Discrete Ordinate Method (DOM). This result is used as the reference solution. Three approximate radiative heat transfer models are also considered. The models are the Planck mean-absorption coefficients for soot, the Planck-mean absorption coefficients for both soot and gas, and the OTA model.

Numerical Model

The overall continuity equation, the Navier–Stokes equations in the low Mach number formulation, and the transport equations for gas-phase species mass fraction, the soot mass fraction, the soot number density per unit mass of mixture, and energy [12] were solved in the 2D rectangular coordinates system (x,z) using a finite

[*] Corresponding author: jean-louis.CONSALVI@univ-amu.fr

volume method on a staggered grid. The correction diffusion velocities in both the x- and z-directions were used to ensure that the mass fractions of gaseous species and soot sum to unity. The thermophoretic velocities of soot in both the x- and z-directions were accounted for, as were the interactions between the gas-phase chemistry and the soot chemistry. The diffusion terms in the transport equations were discretized by the central difference and the convection terms by the power law scheme [13]. The SIMPLE algorithm [13] was used to treat the pressure and velocity coupling. The conservation equations of gas-phase species were solved in a fully coupled fashion at each control volume using a direct solver to ensure the convergence process. All other transport equations are solved using the tridiagonal-matrix algorithm. A relatively short kinetic mechanism developed by Slavinskaya and Frank [14] to predict the formation of PAH and their growth up to five aromatic rings was used in present work. It consists of 94 species and 723 reactions. The radiative source term in the transport equation of energy was computed by DOM coupled to a SNBCK-based wide-band model for the absorption coefficients CO, CO_2, and H_2O [15]. Soot particles were assumed to be spherical and much smaller than wavelengths relevant to thermal radiation (predominately in the near-infrared), so the spectral absorption coefficient of soot was obtained as $5.5 f_S/\lambda$ based on Rayleigh's theory for small particles and the refractive index of soot of Dalzell and Sarofim [16], with f_S being the soot volume fraction and λ the wavelength at the band center. The soot model is on the whole the same as that used by Guo et al. [12] and Consalvi et al. [17] and the soot kinetics is mainly based on the work of Apple et al. [18]. However, two major differences have been introduced as compared to the study reported in Ref. 17. The steric factor for the HACA process is now a constant set equal to 0.1 to be similar to those used in the works of Slavinskaya and coworkers [14, 19, 20]. The contribution of surface growths due to PAH-surface condensation has been added.

Results and Discussions

Computational details

Two-dimensional numerical calculations were performed on a domain of 250 mm (x) × 190 mm (z). A constant mesh size zone of 0.9 x 0.75 mm^2 was used in the flaming region. In the rest of the computational domain a non-uniform mesh was implemented. The total number of cells was 169 (x) × 93 (z). For the flames considered, the fuel and air were injected according to the experimental conditions of Fuentes et al. [9] with a velocity of 3 mm/s and 250 mm/s, respectively. Flat velocity profiles were considered. The injection temperature was 300 K and the effects of fuel preheating were neglected. Pressure was set at 1 atm.

Different radiation models

Six radiation models were considered: (i) the standard SNBCK-wide band model described in the numerical model section. This model was used as reference model to test the other approximations and will be denoted as the reference solution hereafter. (ii) Disregarding the radiative contribution of both participating gases and soot (no radiation), (iii) disregarding the radiative contribution of soot (no soot radiation), (iv) assuming soot is a gray species by using its Planck-mean absorption coefficient. This model will be referred as gray soot in the following, (v) assuming both soot and participating gases are gray species. The Planck-mean absorption coefficient was considered for each radiating species. This model will be denoted as Planck mean hereafter. To be consistent with the reference model, the Planck-mean absorption coefficients considered in models iv and v are computed from the SNBCK wide-band model. It should be pointed out that the differences between gray soot and Planck mean results from the spectral dependence of gaseous radiatively participating species, namely CO, CO_2 and H_2O. (vi) The Optically-Thin Approximation (OTA) where the reabsorption of both participating gases and soot is neglected.

Flame geometry

This section investigates the influence of radiation model on the flame geometry. A special attention is paid to the flame quenching at the flame trailing edge. The flame contour was delimited by the temperature iso-contour of 1400 K. This temperature has been selected for two reasons. First, it corresponds approximately to the temperature below which soot ceases to be oxidized and can then be considered as an indicator of the luminous flame. Secondly, it is close to the extinction temperature of 1500 K ± 50 K proposed by Williams [21] for hydrocarbon combustion in oxygen/nitrogen mixtures.

Figure 1 shows the flame contours calculated using the different radiation models investigated. In the case of the reference model the combustion efficiency, defined as the ratio between the actual heat release rate and that in the case of a complete combustion, is 85% indicating that the flame quenches at the trailing edge before of fuel is fully burnt. The theoretical radiant fraction, defined as the ratio of the radiative loss to the heat release rate in the case of a complete combustion is 0.61. This radiant fraction is substantially higher than those observed in normal gravity laminar axisymmetric flames and is more in line with those computed in microgravity laminar axisymmetric flames [6]. In the reference solution, the flame length (L_f) is 16.55 cm and the flame stand-off distance at the trailing edge is 2.81 cm.

The simulation carried out with no radiation probes that the influence of radiation cannot be neglected in this type of flames. The flame geometry is completely modified as compared to the reference case. Firstly, it is much larger due to higher temperature and then thermal expansion. Secondly, the flame is much taller since no quenching occurs at the trailing edge. In the present case the flame tip occurs outside of the computational domain. Ignoring the participation of soot in radiation computation also results in higher temperature which

leads to a much larger and longer flame than that found the reference case. The flame tip occurs also outside of the computational domain and no conclusion can be then drawn about the completeness of the combustion process.

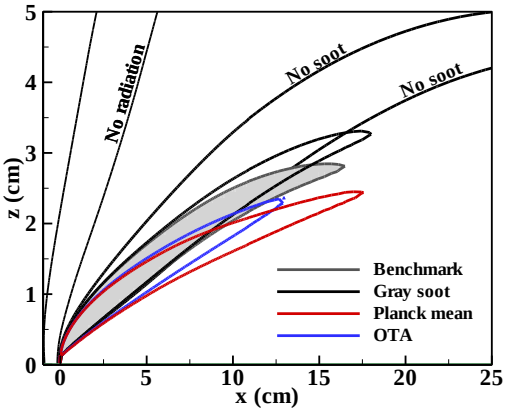

Fig. 1. Flame shape for the different radiation models.

This highlights the importance of the continuous radiation of soot, which represents approximately 45% of the total radiative loss in this problem.

Computation with gray soot (black solid line) and Planck mean (red solid line) models result in longer flame lengths than for the reference case. Flame length is increased from 15.82 cm for complete case to 18.06 cm and 17.62 cm for gray soot and Planck mean cases, respectively. The influence of these approximate radiative models is also pronounced on the stand-off distance at the flame tip which is increased from 2.81 cm (reference case) to 3.27 cm for gray soot model and decreased to 2.45 cm for Planck model. In addition, the combustion efficiency is reduced to 76% as compared to 85% for the reference radiation model. As a consequence, the OTA enhances the radiative losses as compared to the reference case and, as a consequence, favors flame quenching at the trailing edge. This results in a significantly shorter flame of about 12.85 cm, showing that this approximation leads to significant errors.

The phenomenon of flame quenching at the trailing edge laminar boundary layer flames in microgravity is a typical case of radiative extinction. The previous comparison revealed that the significant contribution of soot radiation on this phenomenon. As a consequence only the influences of the approximate models iv) to vi) on flame temperature and soot formation will be discussed in the following.

Let us first consider the flame temperature. Figures 2b, c and d display the distribution of errors in the predicted flame temperature by considering the gray soot, Planck-mean and OTA models, respectively. The error was defined as the difference between the temperature computed with the approximate model and that calculated with the reference model in Fig. 2a ($\Delta T=T_{model}-T_{ref}$). Figure 2b shows that the error for the gray soot model presents four clear quadrants along the

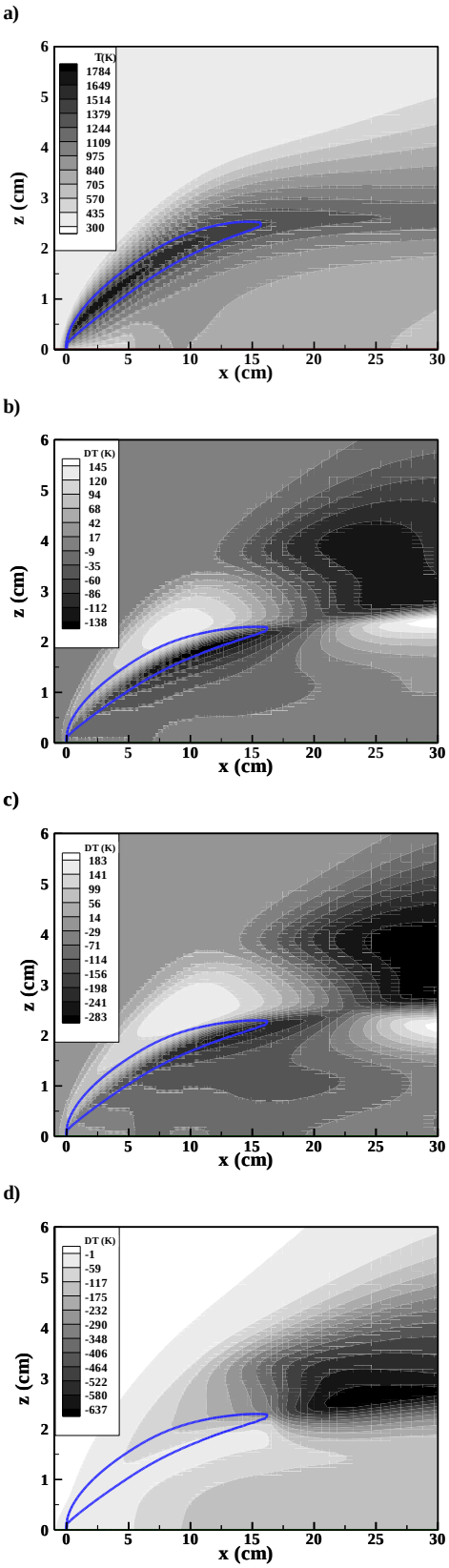

Fig. 2. Distributions of the reference temperature distribution and temperature error predicted using approximate radiation models, (a) temperature distribution of the reference model, (b) error of the Gray soot, (c) error of the Planck mean, and (d) error of OTA.

flame. Between the flame leading edge and the flame tip the gray soot model overpredicts the temperature in the region above the flame reaction zone with a maximum discrepancy of 135 K. On the other hand, the gray soot model underestimates the temperature below the flame reaction zone with a maximum discrepancy of 138 K. Beyond the flame tip, the trend observed previously is inverted with an overpediction in the region between the plate and the stand-off distance. These results show clearly that the spectral dependence of soot has to be taken into account.

The second approximate model, namely the Planck mean, presents qualitatively the same trends as the gray soot model. However, larger discrepancies are observed with maximum over- and under-predictions of 183 K and 283 K, respectively. Comparison with the discrepancies observed in the case of gray soot allows to quantifying the influence of the spectral dependence of gaseous participating species. Eventually, the OTA underpredicts temperature essentially everywhere in the computational domain. This is expected since the absorption of radiation is neglected. In the region between the plate and the flame contour, the discrepancies are found to increase as the distance along the plate increases. The maximum discrepancies occur upstream the flame tip and are of about 637 K, indicating that the effect of radiation absorption of this part of boundary laminar diffusion flame is very important.

On the other hand, is important to study the effects of soot volume fraction in the extinction zone, the results were presented in the Fig. 3. The figures display the distributions of the relative error for the soot volume fraction. The same definition of the relative error as Liu and coworkers [22] is adopted:

$$E_{r,f_S} = \left(f_{S,\mathrm{model}} - f_{S,ref}\right) / f_{S,\max} \qquad (1)$$

where $f_{S,max}$ is the maximum value of the soot volume fraction over the entire computational domain. An analysis of the mechanism leading to soot formation in laminar boundary layer flame has revealed that soot was produced in a region following the stand-of distance. The soot particles were then transported along streamlines inside the boundary layer by convection and thermophoresis (see Fig. 3a) [23]. As a consequence, the distribution of soot inside the boundary layer depends on both the soot formation processes and the flow dynamic. Previous results have shown that the use of approximate radiative models affects, on one hand, the temperature field which has a direct influence on the soot production processes and, on the other hand, the flame geometry which influences the flow dynamic. As a consequence, the relative error on soot volume fraction results from these two effects. Figs. 3b to 3d, showing the relative error in soot volume fraction predicted by the gray soot model, the Planck mean model, and the OTA, respectively, indicate that the distributions of the relative error are similar. These simplified radiation models significantly overpredict the soot volume fraction in most of the region where soot is located, with the maximum relative error being 44%, 87%, and 94% for the gray soot, Planck mean and OTA models, respectively. However, beyond the flame tip (temperature contour of 1400K) and just below the

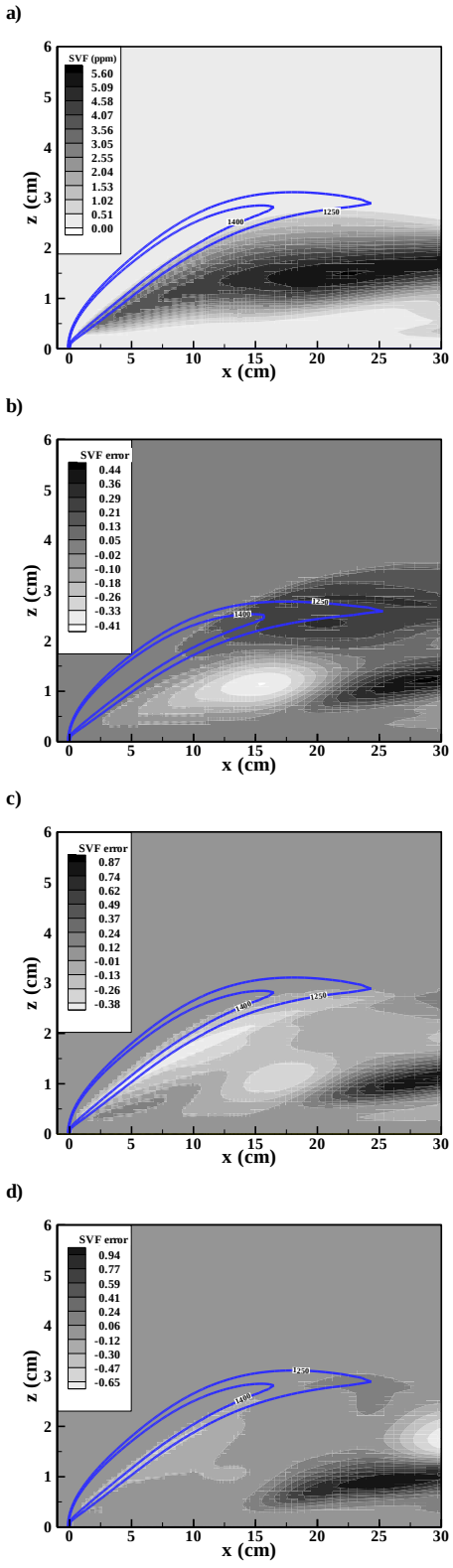

Fig. 3. Distributions of the reference soot volume fraction the relative error of soot volume fraction, (a) soot volume fraction distribution of reference model, (b) Gray soot, (c) Planck mean and, (d) OTA.

stand-off distance, these approximate models lead to a substantial underprediction of the soot volume fraction, with the maximum relative error being 53%, 84%, and 89% for the gray soot, Planck mean, and OTA models, respectively.

The integrated soot volume fraction as a function of the x-coordinate is a measure of the total amount of soot present at a given x-coordinate and is computed using the following expression:

$$F_v(x) = \int_0^{\infty} f_S(x,z)dz \qquad (2)$$

The computed results using the SNBCK wide band model and the three approximate models are compared in Fig. 4. The radiation model affects significantly the integrated soot volume fraction beyond the position of about x = 5 cm, which is consistent with the trend observed in Fig. 3. Between x ≈ 5 cm and ≈ 15 cm all approximate radiation models underpredict the integrated soot volume fraction, which is also consistent with the behavior observed in Fig. 3. The gray soot, Planck mean, and OTA models overpredict the peak integrated soot volume fraction by about 33, 20, and 49%, respectively.

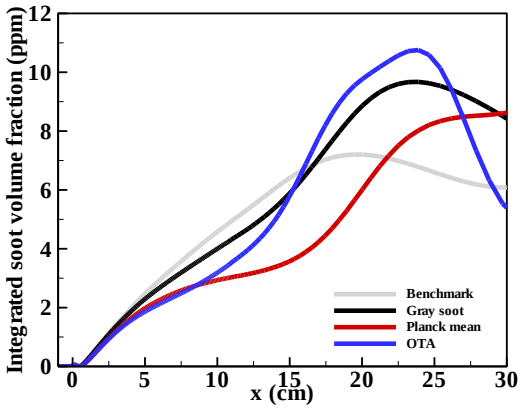

Fig. 4. Distributions of the integrated soot volume fraction as a function of the x-coordinate.

Conclusions

Detailed numerical calculations were conducted in a laminar boundary layer ethylene diffusion flame at microgravity and atmospheric pressure. Three radiation modeling approaches were compared with a reference solution obtained with a SNBCK wide band model coupled to the discrete ordinate method to solve the radiative transfer equation: i) gray soot model with the soot absorption coefficient being its Planck mean, ii) Planck mean with the absorption coefficient of soot and gas mixture being its Planck mean , iii) the Optically-Thin Approximation (OTA). The following conclusions can be drawn:

1. The combustion efficiency is significantly less than 1, indicating that flame quenches at the trailing edge.
2. Soot radiation accounts for 45% of the total radiative heat loss in this flame and plays a significant role in the phenomenon of flame quenching at the trailing edge.
3. Gray soot and Planck mean models cause significant discrepancies in temperature and soot volume fraction distributions and moderate discrepancies in the flame shape. The level of error is higher for the Planck mean model.
4. OTA neglects the absorption of radiation which affects significantly the temperature, the soot volume fraction and the flame shape, and the radiative quenching at the flame tip.

Acknowledgements

J. Contreras wishes to thank the CONICYT Chile for financial support through its “Advanced Human Capital Formation” program.

References

[1] Q. Wang, B.H. Chao, Combust. Flame 158 (2011) 1532-1541.

[2] K.J. Santa, B.H. Chao, P.B. Sunderland, D.L. Urban, D.P. Stocker, R.L. Axelbaum, Combust. Flame 151 (2007) 665-675

[3] S.L. Olson, J.S. T’ien, Combust. Flame 121 (2000) 439-452.

[4] C.M. Megaridis, B. Konsur, D.W. Griffin, Proc. Combust. Inst. 26 (1996) 1291-1299.

[5] J.L. Torero, T. Vietoris, G. Legros, P. Joulain, Combust. Sci. Technol. 174 (2002) 187–203.

[6] G.M. Faeth, Microgravity Combustion, Fire in Free Fall, 1st Edition, Ed. H. Ross, Academic Press, UK, 2001.

[7] G. Legros, A. Fuentes, S. Rouvreau, P. Joulain, B. Porterie, J.L. Torero, Proc. Combust. Inst. 32 (2009) 2461-2470.

[8] G. Legros, P. Joulain, J.P. Vantelon, D. Bertheau, A. Fuentes, J.L. Torero, Combust. Sci. Technol. 178 (2006) 813-835.

[9]A. Fuentes, G. Legros, A. Claverie, P. Joulain, J.P. Vantelon, J.L. Torero, Proc. Combust. Inst. 31 (2007) 2685-2692.

[11] A.C. Fernandez-Pello, D.C. Walther, J.L. Cordova, T. Steinhaus, J.G. Quintiere, J.L. Torero, H. Ross, Space Forum 6 (2000) 237-243.

[12] H. Guo, F. Liu, G.J. Smallwood, Ö.L. Gülder, Combust. Flame 145 (2006) 324-338.

[13] S.V. Patankar, Numerical Heat Transfer and Fluid Flow, Hemisphere, New York, 1980.

[14] N.A. Slavinskaya, P. Frank, Combust. Flame 156:1705-1722 (2009).

[15] F. Liu, G.J. Smallwood, Ö.L. Gülder, J. Thermophys. Heat Transf. 14 (2000) 278-281.

[16] W.H. Dalzell, A.F. Sarofim, J. Heat Transfer 91 (1969) 100–104.

[17] J.L. Consalvi, J. Contreras, A. Fuentes, F. Liu, F., 8th Mediterranean Combustion Symposium, Cesme, Turkey, 2013.

[18] J. Appel, H. Bockhorn, M. Frenklach, Combust. Flame 121 (2000) 122-136.
[19] S.B. Dworkin, Q. Zhang, M.J. Thomson, N.A. Slavinskaya, U. Riedel, Combust. Flame 158 (2011) 1682-1695.
[20] V. Chernov, M.J. Thompson, S.B. Dworkin, N.A. Slavisnkaya, U. Riedel, Combust. Flame 161 (2014) 592-601.
[21] F.A. Williams, Fire Safety J. 3 (1981) 163-175.
[22] F. Liu, H. Guo, G. Smallwood, Combust. Flame 138 (2004) 136-154.
[23] J. Contreras, J.L. Consalvi, A. Fuentes, F. Liu, to be presented in 9th Mediterranean Combustion Symposium, Rhodes, Greece, 2015.